Effect of hydraulic retention time on continuous electricity production from xylose in up-flow microbial fuel cell

Johanna M. Haavisto[1,*], Marika E. Kokko[1], Chyi-How Lay[2,3], Jaakko A. Puhakka[1]

[1] Laboratory of Chemistry and Bioengineering, Tampere University of Technology, Tampere, Finland

[2] Green Energy Development Center, Feng Chia University, Taichung, Taiwan

[3] Master's Program of Green Energy Science and Technology, Feng Chia University, Taiwan

* Corresponding author: P.O. Box 541, FI-33101 Tampere, Finland; E-mail: johanna.haavisto@tut.fi; Telephone: +358400486070

Abbreviations

CE	Coulombic efficiency (%)
COD	Chemical oxygen demand
DGGE	Denaturing gradient gel electrophoresis
HRT	Hydraulic retention time (d)
MFC	Microbial fuel cell
OLR	Organic loading rate (g/L/d)
PCR	Polymerase chain reaction
SL	Sequence length
UV	Ultraviolet
VFA	Volatile fatty acid

Abstract

Aerobic wastewater management is energy intensive and, thus anaerobic processes are of interest. In this study, a microbial fuel cell was used to produce electricity from xylose which is an important constituent of lignocellulosic waste. Hydraulic retention time (HRT) was optimized for the maximum power density by gradually decreasing the HRT from 3.5 d to 0.17 d. The highest power density (430 mW/m^2) was obtained at 1 d HRT. Coulombic efficiency decreased from 30% to 0.6% with HRT's of 3.5 d and 0.17 d, respectively. Microbial community analysis revealed that anode biofilm contained known exoelectrogens, including *Geobacter* sp and fermentative organisms were present in both anolyte and the anode biofilm. The peak power densities were obtained at 1-1.7 d HRTs and xylose degraded almost completely even with the lowest HRT of 0.17 d, which demonstrates the efficiency of up-flow MFC for treating synthetic wastewater containing xylose.

Keywords

Microbial fuel cell, xylose, continuous operation, up-flow, hydraulic retention time, microbial community

1. Introduction

Sustainablity in wastewater management requires energy and performance efficiencies. The energy-rich compounds in wastewater should be converted to useful energy. One possibility to recover energy from wastewaters is production of electricity using microbial fuel cells (MFCs) [1,2]. In MFCs, microorganisms oxidize wastewater constituents and convert their chemical energy into electricity with simultaneous wastewater purification [3].

In Finnish paper, cardboard and pulp mills, in 2013, approximately 500 Mm^3 of wastewater was produced [4] containing cellulose and hemicellulose. Glucuronoxylans with xylose as the most abundant monomer, are hemicellulose that is present in high concentrations especially in hardwood [5]. The occurrence of hemicellulose and thus, xylose in forest industry wastewaters decreases the cost-effectiveness of the treatment process if xylose is not degraded [6]. For example, a yeast *S. cerevisiae* cannot utilize xylose for bioethanol production without gene modification [7]. However, it has been reported that in MFCs xylose can be anaerobically converted to electricity [8,9,10,11].

Continuous treatment is a prerequisite for efficient and low-cost wastewater treatment. Only a few studies have reported continuous electricity production from xylose [8,10]. In continuous operation, organic loading rate (OLR) has a remarkable effect on electricity production [12] and the OLR is controlled by the HRT used. By now, several different reactor configurations have been tested for simultaneous electricity production and wastewater treatment, from which up-flow reactors are easily scalable and have comparatively low space requirements and thus, have potential for future applications [12,13,14,15,16]. Up-flow reactors can be operated with high OLRs [17], i.e. low HRTs, and to treat wastewaters containing compounds, such as phenol [18]. Recently, granular activated carbon (GAC) has been reported at the MFC anodes to increase the surface area and performance of anodes as well as their wastewater treatment efficiency [19,20]. GAC can be

combined with up-flow reactors, i.e. fluidized bed reactors [21], which further highlights the importance of up-flow configuration for bioelectrochemical systems in the future. [20] To make MFCs economically feasible for wastewater treatment, the treatment time should be close to the conventional processes. This makes HRT an important operational parameter [22].

This study examined the effects of HRT and organic loading rate on the ability of an up-flow MFC to convert xylose to electricity by further optimizing the operation parameters reported by Lay et al. [10]. The COD removal efficiencies and microbial communities at the anolytes were determined for each tested HRT. In addition, the microbial community of the biofilm was characterized in the end of the experiment.

2. Materials and Methods

2.1 MFC construction and operation

The up-flow MFC used was similar to the one used by Lay et al. [10]. Anode and cathode chambers (working volumes 500 mL and 250 mL, respectively) of dual-chambered up-flow MFC (Figure 1) were separated with an anion exchange membrane (Ø 4.5 cm, AMI-7001, Membranes International Inc. USA). The membrane was changed on days 23, 78, 117, 132, and 159 due to membrane fouling. Flat plate graphite electrodes at the anode and cathode (0.00385 m^2, McMaster-Carr, Aurora, OH) and 100 Ω external resistance were used [10]. A reference electrode (Ag/AgCl in 3M KCl solution, -205 mV vs. standard hydrogen electrode (SHE), SENTEK QM710X) was attached to the anode recirculation tubing on day 15 through a glass capillary (QiS, the Netherlands). Anolyte temperature was maintained at 37 °C with heating coils around the anode chamber. Temperature was measured from the circulated anolyte which had a flow rate of 60 mL/min [10]. Medium was prepared as described by Mäkinen et al. [23] without addition of EDTA, yeast extract,

and resazurin. Xylose (0.5 g/L) was used as substrate and pH of the medium was adjusted to 7.0 with NaOH before feeding. During continuous operation, influent container was kept in a cool box (approximately 9 °C) to minimize microbial growth outside the reactor. The catholyte was potassium ferricyanide (50 mM $K_3Fe(CN)_6$) in phosphate buffer (100 mM Na_2HPO_4, pH 7.0). Catholyte was circulated after day 83 through a container (500 mL) with a minimum flow rate of 0.2 mL/min. MFC was started as fed-batch where 0.5g/$L_{\text{anode chamber volume}}$ xylose was added with an interval of 4-7 days. Continuous operation was started on day 43 with 3.5 d HRT, and HRT was gradually decreased to 0.17 d. Inoculum [10] was originally enriched from a compost culture.

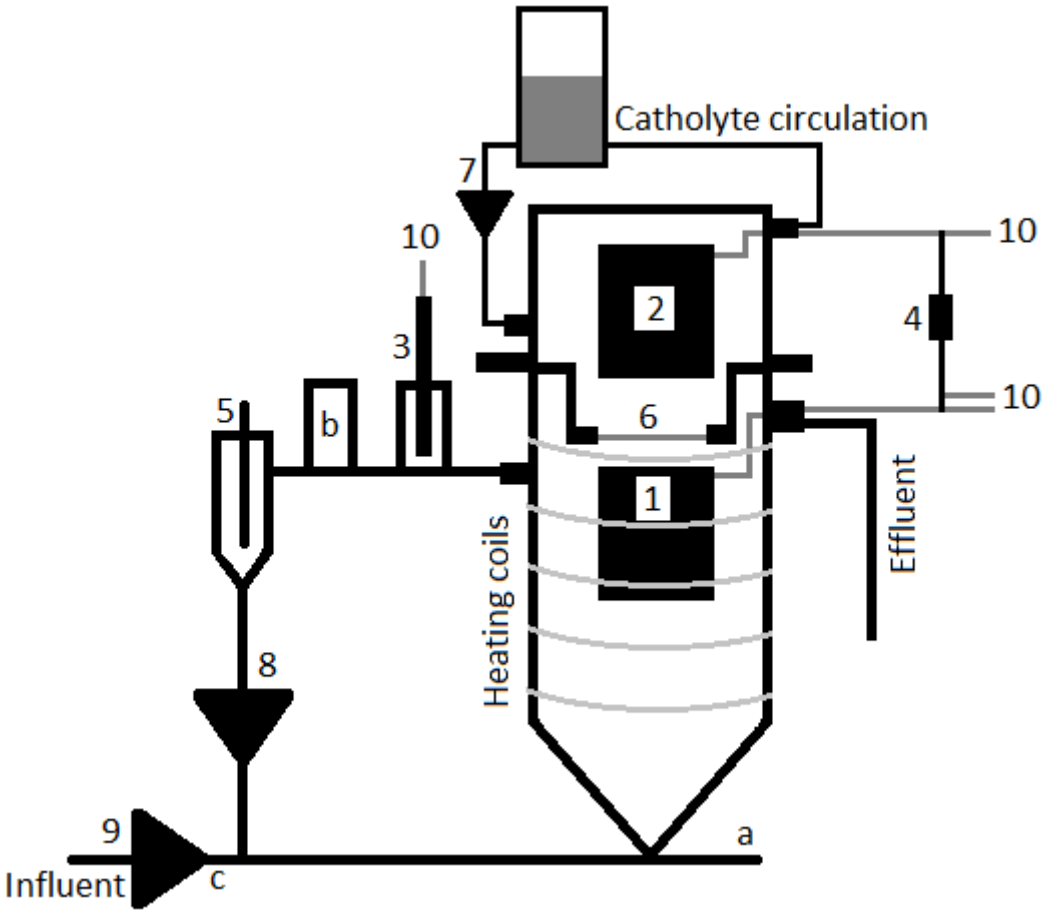

Figure 1. Diagram of MFC construction. 1) Anode electrode, 2) Cathode electrode, 3) Reference electrode, 4) External resistance, 5) Temperature sensor, 6) Anion exchange membrane, 7) – 9)

Peristaltic pumps, 10) Electrical wires connected to data logger, a) - c) Sampling ports. The figure is not drawn to scale.

2.2 Analyses

2.2.1 Electrochemical measurements and calculations

Cell voltage and anode potential were measured at 2 min intervals with an Agilent 34970A data Acquisition/Switch Unit (Agilent, Canada). The current was calculated from cell voltage (U) and external resistance (R) with ohm´s law. Current and power densities were calculated against the projected area of the anode electrode (0.00385 m^2) or the volume of the anode chamber ($0.5*10^{-3}$ m^3).

Performance analyses were performed at the end of each HRT by measuring cell voltage and anode potential after 30 min of stabilization with different external resistances (1000 Ω, 499 Ω, 240 Ω, 100 Ω, 10 Ω) and at open circuit mode. Power density and polarization curves were drawn from performance analyses results. Internal resistances were further estimated from the slopes of polarization curves according to [24].

Coulombic efficiency (CE) was calculated at each HRT using the measured cell voltage and the added influent xylose concentration over the periods with stable cell performance according to Equation 1

$$C_E = \frac{M_s \int_{t_1}^{t_2} \frac{U}{R} dt}{F b_{es} \frac{t_b v_a}{HRT} c}, \quad (1)$$

where M_s = molecular weight of xylose (g/mol), t_2-t_1 = time period of the measurement (d), F = Faraday's constant (96 485 C/mol*e), b_{es} = number of the electrons released per mol of xylose (20 e^-), v_a = working volume of anode chamber (L), HRT = hydraulic retention time (d) and c = xylose concentration (g/L).

2.2.2 Sampling and chemical analysis

Xylose concentration, pH, and volatile fatty acids (VFAs) and alcohols were analyzed 3 times a week. During batch mode operation, samples were taken from sample port a (Figure 1) before substrate was added. During continuous operation, samples were taken from sample port b (Figure 1) and from effluent and influent. Samples for VFA, ethanol and xylose analysis were filtered through 0.2 or 0.45 μm PET filter. WTW pH 330 meter was used for measuring pH.

Xylose concentration was measured with phenol-sulphuric acid method [25] using customized sample and reagent volumes (1 mL sample, 0.5 mL 5% phenol solution, and 2.5 mL sulphuric acid) and measuring the absorbance at 485 nm with UV-visible spectrophotometer (Shimadzu UV-1601). VFAs and alcohols were measured with a gas chromatograph (Shimadzu Ordior GC-2010 plus) equipped with ZB-WAXplus column (Phenomenex, USA) and flame ionization detector (FID). The oven temperature was held at 40 °C for 2 min, increased 20 °C/min to 160 °C, and 40 °C/min to 220 °C, where the temperature was held for 2 min. Temperature of injector and detector was 250 °C. The flow of helium (carrier gas) was 30 mL/min. Internal standards were crotonic acid (100 mg/L) and 1-propanol (60 μL/L), and 0.06 M oxalic acid solution was used to acidify the samples.

COD removal was calculated by converting the analysed effluent VFAs and xylose concentrations to COD equivalents according to van Haandel & van der Lubbe [26].

2.2.3 Microbial community analyses

Microbial community samples were obtained from the anodic solution at each HRT at stabilized conditions and from the anode biofilm in the end of the experiment. The biofilm sample was removed from the anode electrode by sonicating 5 min in 0.9% NaCl solution, followed by further separation of biomass with a centrifuge (5000 x g, 10 min). DNA was extracted from defrosted pellets with PowerSoil DNA isolation kit (MO BIO Laboratories, Inc., Carlsbad, CA, USA). PCR was used to amplify partial 16S rRNA genes as described by Koskinen et al. [27] using GC-BacV3f [28] and 907r [29] primers. DGGE was performed as described by Lakaniemi et al. [30]. Separated DNA sequences were reamplified according to Koskinen et al. [27] before sequencing at Macrogen Inc. (Seoul, Korea). BioEdit software and BLAST (http://blast.ncbi.nlm.nih.gov/Blast.cgi) were used for analyzing sequence data.

3. Results and discussion

3.1 Electricity generation

Electricity production with the studied up-flow microbial fuel cell was mainly affected by the changes in HRT. The effects of other variables, such as fast reduction of catholyte and changes in internal resistance caused by membrane fouling, were minimized by circulating the catholyte and by changing the membrane periodically, respectively (Figure A2). During reactor operation, cell voltage increased from 344 mV to the highest value of 408 mV when HRT was decreased from 3.5 d to 1 d. Decreasing HRT to 0.75 d and further to 0.17 d decreased the cell voltage remarkably to 218 mV and 156 mV, respectively (Figure A2). Similar trend was observed in performance analysis (Figure 2), which was done at the end of each HRT.

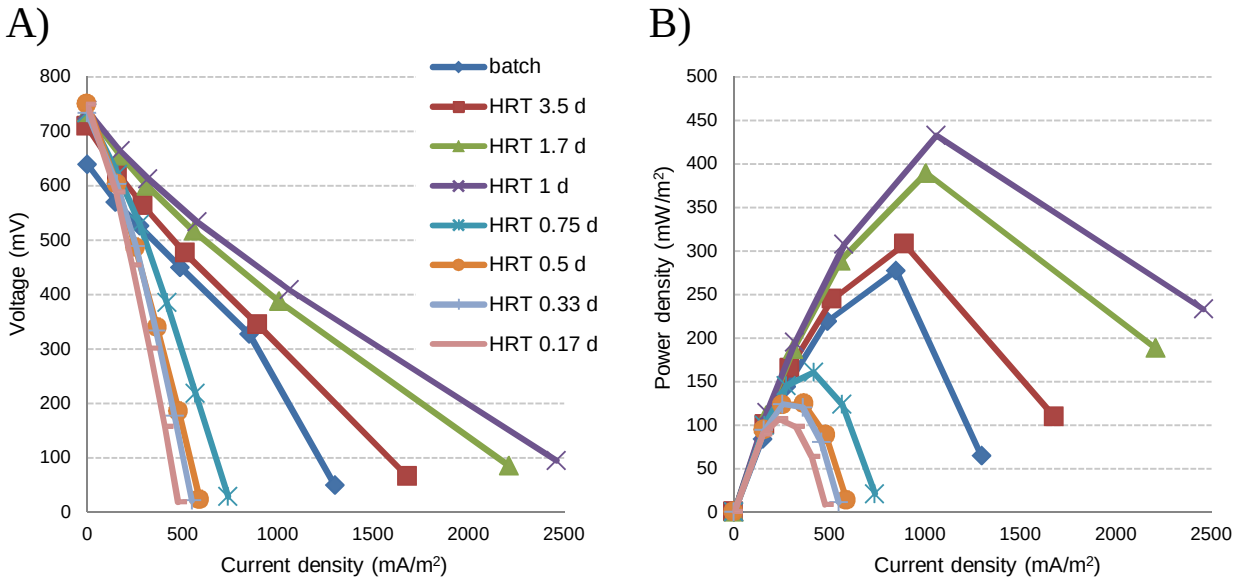

Figure 2. A) Cell voltage and B) power density as a function of current density in the up-flow microbial fuel cell operated with different HRTs.

The highest current density of 2460 mA/m^2 and the highest voltages with all tested external resistances (10-1000 Ω) were obtained with HRT of 1 d (Figure 2A). At HRTs above 1 d the current densities and voltages were lower than at HRT of 1 d. The OLR at HRTs above 1 d was below 0.4 g COD/L/d, which may not have provided enough substrate for the microorganisms to sustain higher voltages [8]. Also decreasing HRT below 1 d decreased the current densities, cell voltages (Figure 2A) and CEs and increased VFA concentrations (Chapter 3.2), which indicates that at lower HRTs the biofilm could not utilize xylose for current production as efficiently as at higher HRTs. Increasing mass transfer or diffusion limitations likely affected the decreasing performance of the cell [31 32].

Internal resistances of the cell were smaller in batch mode (90 Ω) and at HRTs between 1 and 3.5 d (70-90 Ω) and increased remarkably when HRT was decreased below 1 d (270-450 Ω). Ieropoulos et al. [31] and Lee & Oa [17] also found the increase in internal resistance with higher influent flow rates. On reason for this can be insufficient substrate transfer to biofilm and proton transfer into cathode chamber [17] (mass transfer and diffusion limitations), which could be prevented by improving the anode electrode geometry [33] and reactor design. Ieropoulos et al. [31] also suggested that the increase in internal resistance is partly due to the increased microbial growth on anode electrode at lower HRTs resulting in diffusion limitations or due to the changes in microbial community that may have caused mass transfer limitations with higher flow rates. At each HRT of this study, the time reserved for stabilization was at least 10 times the HRT. These periods were long enough for causing changes in biofilm thickness and increasing internal resistance. Although the highest current densities were measured with 1 d HRT, anode potential reached the most negative stable values (with 100 Ω resistance) of -455 ± 2 mV vs. Ag/AgCl with the smallest HRTs of 0.17-0.5 d compared to -416 mV vs. Ag/AgCl at HRT of 1 d (Table 1). This indicates that the

performance of the anodic biofilm did not deteoriate with decreasing HRTs. However, at smaller HRTs the high internal resistances decreased power densities.

The internal resistance of the cell was high (70 Ω, Figure 2) also with the optimal HRT of 1 d indicating that the reactor configuration requires improvements. This could be done, for example, by decreasing the distance between the electrodes [13] and improving the membrane operation, e.g. by increasing the area of the membrane. For example, Sevda et al. [34] reported that the hindered ion flow through a separator between anode and cathode compartments caused more resistance with smaller HRTs in their reactor.

According to the power density curves (Figure 2B), 1 and 1.7 d HRTs resulted in the highest power densities and 1 d HRT gave 11% higher values than 1.7 d HRT. On the other hand, during the stable operation (Figure 3, Figure A2) 1.7 d HRT gave 26% higher power densities than 1 d HRT. When taking into account the variations in cell voltage (Figure A2) caused by the fast reduction of catholyte, xylose consumption in the feeding tank, and membrane fouling, the cell performance at HRTs 1 and 1.7 d was comparable. Thus, both 1 d and 1.7 d are near the optimal HRT for the studied up-flow MFC in relation to the electricity production from synthetic wastewater containing xylose (Figure 3). These are in the same range with the HRTs of the existing activated sludge wastewater treatment plants in pulp and paper mill [35].

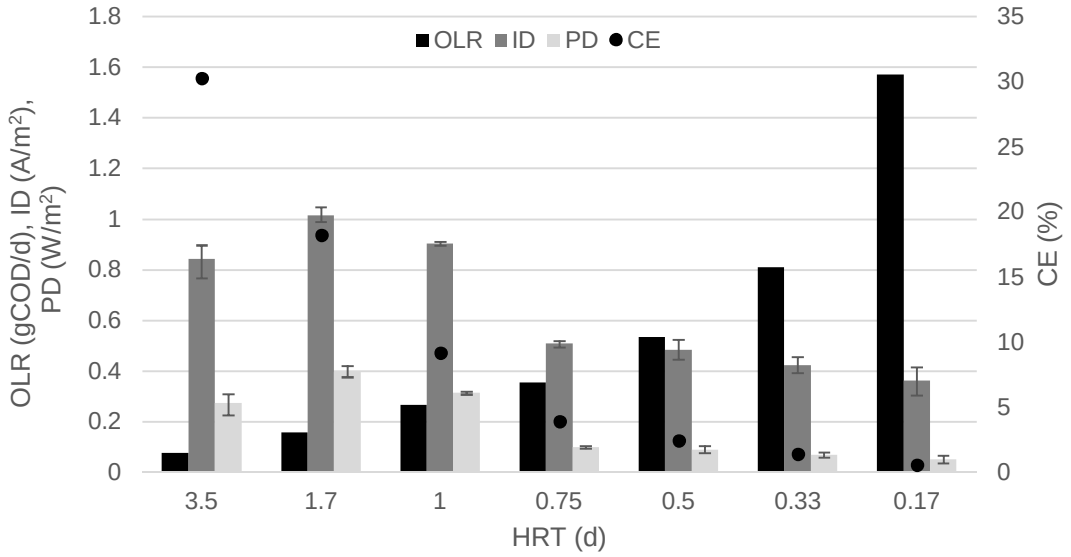

224

225 **Figure 3.** Organic loading rate (OLR, gCOD/d), average current density (ID, mA/m^2), power
226 density (PD, mW/m^2) and Coulombic efficiency (CE, %) as a function of hydraulic retention time
227 (HRT, d) in up-flow microbial fuel cell. The error bars show the minimum and maximum values in
228 stable conditions.

229

230 The peak power densitiy obtained at 1 d HRT is significantly higher than 8.4 ± 0.4 mW/m^2 reported
231 by Huang et al. (Table 1) with xylose. They suggested that low power densities were due to non-
232 optimal cultivation conditions. Huang & Logan [8] measured 1093 ± 43 mW/m^2 (against projected
233 surface of cathode electrode) for continuous process fed with xylose (3 g/L). This value was 150%
234 higher than the maximum power density in our study, but their estimated anode electrode surface
235 was approximately 300 times higher than the cathode electrode area resulting in unreliable
236 comparison.

237

Reactor	Xylose feeding concentration	Max. Power density (mW/m^2)	CE (%)	Reference
Air cathode MFC	3 g/L (fed-batch) in 100 mM PBS	673 ± 43[a]	n.g.	[8]
Air cathode MFC	3 g/L (fed-batch) in 200 mM PBS	944 ± 32[a]	n.g.	[8]
Air cathode MFC	3 g/L (continuous); 0.83 d HRT	1093 ± 43[a]	41	[8]
Up-flow; two-chamber	0.5 g/L (fed-batch)	107	21.3 ± 1.0	[11]

Up-flow; two-chamber	0.5 g/L (continuous); 3.5 d HRT	72	12.7 ± 0.6	[11]
Up-flow; two-chamber	0.5 g/L (continuous); 1 d HRT	430	9.2	This study
Two-chamber system	0.08 g/L (fed-batch)	2.6 ± 0.2	41 ± 1.6	[31]
Two-chamber system with stirring	1.5 g/L (fed-batch)	8.4 ± 0.4	36 ± 1.2	[31]

238 [a] normalized to cathode electrode area, n.g.=not given

239 Table 1. Maximum power densities and coulombic efficiences measured in this study and reported
240 in literature.Maximum power density is normalized to anode electrode area unless otherwise stated.

241

242 CEs (calculated from the stable operational period, Figure A2) decreased with HRT during the
243 whole experiment (Table 1). The highest CE of 30% measured with 3.5 d HRT was remarkably
244 higher than reported by Lay et al. ([10] in Table 1) in the same reactor configuration as used in this
245 study. Furthermore, power density with 3.5 d HRT measured in this experiment was three times
246 higher compared to the results of Lay et al. [10] with the same HRT. One reason for the better CE
247 and power density in this experiment can be the longer acclimation time, which helps bacteria to
248 adapt to the operational conditions. Also regular membrane changes due to membrane fouling might
249 have improved the results of this experiment, since they decreased the internal resistance. For
250 example, with 1 d HRT, membrane change improved the cell voltage by 17% (measured one day
251 after the membrane change). Later with smaller HRTs the differences were even higher (Figure A2)
252 indicating that smaller HRT increased membrane fouling. Huang & Logan [8] were able to
253 transform 13-40 % of the chemical energy of the removed xylose (initial concentration 20 mM =
254 3.0 g/L) into electricity with HRTs of 10-38 h. They used graphite fiber brushes as anodes which
255 enabled a larger surface area and lower internal resistance (2-3.4 Ω) than used in this study. Thus,
256 decreasing the internal resistance in the reactor configuration of this study will likely increase CE
257 and power densities.

258

259 The purpose of this study was to examine the effects of different HRTs to the performance of the
260 anode. To further optimize the economical feasibility of the process, different anode electrode

materials and structures should be tested. Also reactor configuration optimization is needed for more efficient electricity production. Potassium ferricyanide is a very good electron acceptor for studying reactions at anode chamber. For practical application, however, this has to be replaced with an inexpensive and environmental friendly choice, such as efficient cathode based on O_2 reduction.

3.2 Metabolic activity in up-flow MFC

On average, 99% of the xylose was removed at the anode during the continuous reactor operation. The xylose removal was very efficient even with the lowest HRT of 0.17 d compared to the other MFC studies with continuous xylose feeding. For example, in the studies of Huang and Logan [8] 51-96% of xylose was degraded with HRTs of 5-38 h. However, the influent xylose concentration was lower in our study, which might have affected removal efficiency.

The COD removal calculated from the effluent VFAs and xylose concentrations varied between 57-95% due to remaining VFAs in effluent (Table 2). Propionate remained below 0.5 mM during the reactor run, while the acetate increased with decreasing HRT (2.9 ± 0.6 mM at 0.75 d HRT). With lower HRTs than 0.75 d, the acetate concentrations decreased with HRT. The VFA concentrations fluctuated as indicated by high standard deviations in Table 2.

HRT	anode potential (mV vs. Ag/AgCl)	CE (%)	acetate (%)	propionate (%)	xylose (%)	calculated COD removal (%)
3.5	-410	30.3	< 6	<10	3.1 ± 2.6	95
1.7	-383	18.2	8.3 ± 6.6	8.6 ± 5.2	<2	82
1	-417	9.2	21.7 ± 10.1	9.4 ± 3.5	<2	69

0.75	-444	3.9	35.1 ± 7.6	7.0 ± 2.4	<2	57
0.5	-455	2.5	30.2 ± 10.5	<10	<2	68
0.33	-455	1.5	22.5 ± 3.1	n.d.	<2	77
0.17	-455	0.6	21.6 ± 8.5	n.d.	<2	78

n.d. = not detected

Table 2. Stable anode potentials with different HRTs and electron balance of the added xylose divided to CE and acetate, propionate and xylose measured from the effluent. Detection limit for VFAs was 0.5 mM. CE was calculated for the stable conditions (S1), but concentrations of VFAs and xylose in effluent were calculated over the whole operation period at each HRT. COD removal was calculated based on the effluent composition.

During batch mode operation, the pH in the reactor decreased to 5.5, at which point it was increased with NaOH to 7.0. During continuous operation, the pH values remained between 6.7-7.1 in the reactor and 6.8-7.4 in the effluent.

3.3 Microbial community analysis

Decreasing HRT will likely wash out some of the bacteria not attached to the biofilm [36]. Thus, the changes in anolyte microbial community were monitored during the experiment. DGGE was used for community profiling although it was realized that it is a semi-quantitative method at best. However, it enables the detection of main bacterial species present at the anolyte. The anolyte microbial communities changed slightly during the experiments. The intensity of the bands on the DGGE gel [27,37] changed at different HRTs indicating that the share of *Cristensenella minuta* increased remarkably after the HRT decreased to 0.5 d (Figure A1, Table 3). *C. minuta* is a xylose fermenting bacterium [38] and its share likely increased due to increased xylose loading rates at

lower HRTs and was related to decreasing power densities and CEs. Fermentative bacteria, being able to degrade xylose, have a role also in electricity production by offering acetate, propionate and butyrate as fermentation end products for exoelectrogenic bacteria [11,39]. However, high substrate concentration increases the growth of fermenting bacteria, thus decreasing power density by overtaking the anolyte and anode electrode biofilm [40]. The share of a nitrate reducing bacterium [41], *Petrobacter* sp., decreased with HRT. With HRTs of 0.17-0.5 d and the most negative anode potentials, the strongest bands belonged to *C. minuta*, *Citrobacter freundii*, *Clostridium indoli*s, and *Proteiniphilum acetatigenes.* All of these bacteria are fermenting, but *P. acetatigenes* cannot ferment D-xylose [38,42,43]. *C. indolis* is a sulfate reducer [44] and *C. freundii* is an exoelectrogenic organism [45]. *C. indolis* has also been found from a biofilm sample of a MFC [37].

The reactor was stopped due to a malfunction in temperature controller, which increased the temperature in the reactor causing heat shock. The microbial community of anode biofilm was characterized after this temperature increase, which possibly affected the results. *Geobacter* sp. was identified from biofilm sample as was also an uncultured *spirochete*, *P. acetatigenes* and *Wolinella succinogenes*. *Geobacter* sp. is a well-known exoelectrogenic organism, but also the uncultured *spirochete* and fermenting *P. acetatigenes* have been found from biofilm of MFC reactors [46,47,48]. Cord-Ruwish et al. [49] found syntrophic cooperation between *W. succinogenes* and *Geobacter* where *W. succinogenes* kept hydrogen partial pressure low, thus helping *Geobacter* to ferment acetate. The increase in effluent acetate concentration with 0.17 -1 d HRTs indicate that acetate oxidation to electricity was the process limiting factor. This was possibly due to liquid flow bypass and the following diffusion and mass transfer limitations between anode biofilm and anolyte flow, which could be improved with more sophisticated anode electrode design.

326

Band label	SL	Sim (%)	Affiliation (acc)	Class / Family	Origin of the sample
1	454 - 481	99.7 - 100	Proteiniphilum acetatigenes (HQ710548.1)	Bacteroidia / Porphyromonadaceae	Crude oil contaminated soil
2	421	99.5	Wolinella succinogenes (NR_025942.1)	Epsilonproteobacteria / Helicobacteraceae	Rumen
3	271 - 444	97.0 - 99.7	Clostridium indolis (KF611981.1)	Clostridia / Lachnospiraceae	Pit mud
4	460 - 538	100	Geobacter sp. (KF006333.1)	Deltaproteobacteria / Geobacteraceae	MFC, inoculated with wastewater
5	461	99.3	Christensenella minuta (AB490809.1)	Clostridia / Christensenellaceae	Isolated from human faeces
6	437	99.7	Clostridium oroticum (AB818947.1)	Clostridia / Lachnospiraceae	Mud
7	262	100	Enterobacter sp. (KF934473.1)	Gammaproteobacteria / Enterobacteriaceae	Sediment samples from PrydzBay and sea area
8	437 - 482	100	Citrobacter freundii (AB680434.1)	Gammaproteobacteria / Enterobacteriaceae	Unknown
9	475	99.5 - 100	Petrobacter sp. (HM059764.1)	Betaproteobacteria / Hydrogenophilaceae	Aerobic enrichment of biodegraded oil sample
10	416	100	Uncultured spirochete (JF736651.1)	Spirochaetia / unknown	MFC, inoculated with activated sludge

327

328 **Table 3.** Identified bands on DGGE gel. SL = sequence length of the sample, Sim (%) = similarity
329 (%), Affiliation (acc) = closest species in database and its accession number, and Origin of the
330 sample = Origin of the sample with the closest match
331
332
333 Fermentative xylose degraders were present in the anolyte and the biofilm contained a known
334 exoelectrogen, *Geobacter sp.* Thus, syntrophic interaction between fermenting and electricity
335 producting bacteria likely took place. *P. acetatigenes, W. succinogenes*, *Petrobacter* sp., uncultured
336 *spirochete*, and *C. freundii* were also present in the anolyte of the reactor from which the inoculum
337 was obtained for this study [10].
338
339
340 # 4. Conclusions
341
342 HRT affected xylose conversion to electricity in up-flow microbial fuel cells as follows: 1) The
343 highest power densities were achieved with 1 d and 1.7 d HRTs, while CE decreased with the HRT
344 from 30% to 0.6%; 2) Xylose was almost completely removed with all HRTs, but due to incomplete
345 acetate oxidation at lower HRTs COD removal remained at 59-95% (70% with 1 d HRT); 3)
346 Microbial communities of anolyte and biofilm contained fermentative bacteria and known
347 electricity producers, respectively. This demonstrates synergistic interaction between xylose
348 fermenting bacteria and exoelectrogens in the biofilm. However, the increasing share of
349 fermentative bacteria with HRTs below 0.75 d likely decreased power density by increasing the
350 internal resistance.
351

Acknowledgement

The Academy of Finland (New Indigo ERA-Net Energy 2014; Project no. 283013) is gratefully acknowledged for financial support. We would like to thank Dr. Aino-Maija Lakaniemi for assistance during writing process.

References

[1] Kokko, M., Mäkinen, A. E. & Puhakka, J. A. 2016. Anaerobes in Bioelectrochemical Systems. Advances in Biochemical Engineering/Biotechnology 156, pp. 263-292.

[2] Butti, S. K., Velvizhi, G., Sulonen, M., Haavisto, J., Köroğlu, E., Çetinkaya, A., Singh, S., Arya, D., Annie Modestra, J., Vamsi Krishna, K., Verma, A., Özkaya, B., Lakaniemi, A-M., Puhakka, J. A. & Venkata Mohan, S. 2016 . Microbial electrochemical technologies with the perspective of harnessing bioenergy: Maneuvering towards upscaling. Renewable and Sustainable Energy Reviews 53, pp. 462-476.

[3] Logan, B. E. 2005. Simultaneous wastewater treatment and biological electricity generation. Water Science & Technology 52, 1-2, pp. 31-37.

[4] Finnish Forest Industry Federation. 2014. Statistics [WWW]. [Cited 16.6.2015]. Available at: http://www.forestindustries.fi/

[5] Willför, S., Sundberg, A., Pranovich, A. & Holmbom, B. 2005. Polysaccharides in some industrially important hardwood species. Wood Science and Technology 39, 8, pp. 601-617.

[6] Groves, S., Liu, J., Shonnard, D. & Bagley, S. 2013. Evaluation of hardboard manufacturing process wastewater as a feedstream for ethanol production. Journal of Industrial Microbiology and Biotechnology 40, 7, pp. 671-677.

[7] Wei, N., Xu, H., Kim, S. & Jin, Y-S. 2013. Deletion of FPS1, Encoding Aquaglyceroporin Fps1p, Improves Xylose Fermentation by Engineered *Saccharomyces cerevisiae*. Applied and Environmental Microbiology 79, 10 pp. 3193-3201.

[8] Huang, L. & Logan, B. E. 2008. Electricity production from xylose in fed-batch and continuous-flow microbial fuel cells. Applied Microbial and cell physiology 80, 4, pp. 655-664.

[9] Mäkinen, A. E., Lay, C-H., Nissilä, M. E. & Puhakka, J. A. 2013. Bioelectricity production on xylose with a compost enrichment culture. International Journal of Hydrogen Energy 38, 35, pp. 15606-15612.

[10] Lay, C-H., Kokko, M. E., & Puhakka, J. A. 2015. Power generation in fed-batch and continuous up-flow microbial fuel cell from synthetic wastewater. Energy 91, pp. 235-241.

[11] Huang, L., Zeng, R. & Angelidaki, J. 2008. Electricity production from xylose using a mediator-less microbial fuel cell. Bioresource Technology 99, 10, pp. 4178-4184.

[12] Hashemi, J. & Samimi, A. 2012. Steady state electric power generation in up-flow microbial fuel cell using the estimated time span method for bacteria growth domestic wastewater. Biomass & Bioenergy 45, pp. 65-76.

[13] He, Z., Minteer, S. D. & Angenent, L. T. 2005. Electricity Generation from Artificial Wastewater Using an Upflow Microbial Fuel Cell. Environmental Science & Technology 39, 14, pp. 5262-5267.

[14] He, Z., Wagner, N., Minteer, S. & Angenent, L. 2006. An Upflow Microbial Fuel Cell with an Interior Cathode: Assessment of the Internal Resistance by Impedance Spectroscopy. Environmental Science & Technology 40, 17, pp. 5212-5217.

[15] Zhao, L. & Song, T. 2014. Simultaneous carbon and nitrogen removal using a litre-scale upflow microbial fuel cell. Water Science & Technology 69, 2, pp. 293-297.

[16] Salar-García, M. J., Ortiz-Martínez, V. M., Baicha, Z., de los Ríos, A. P. & Hernández-Fernández, F. J. 2016. Scaled-up continuous up-flow microbial fuel cell based on novel embedded ionic liquid-type membrane-cathode assembly. Energy 101, pp. 113-120.

[17] Lee, Y. & Oa, S. W. 2014. High speed municipal sewage treatment in microbial fuel cell integrated with anaerobic membrane filtration system. Water Science & Technology 69, 12, pp. 2548-2553.

[18] Jayashree, C., Sweta, S., Arulazhagan, P., Yeom, P., Iqbal, M. & Banu, J. 2015. Electricity generation from retting wastewater consisting of recalcitrant compounds using continuous upflow microbial fuel cell. Biotechnology and Bioprocess Engineering 20, 4, pp. 753-759.

[19] Jiang, D. & Li, B. 2009. Granular activated carbon single-chamber microbial fuel cells (GAC-SCMFCs): A design suitable for large scale wastewater treatment processes. Chemical Engineering Journal 47, pp. 31-37.

[20] Jiang, D., Curtis, M., Troop, E., Scheible, K., McGrath, J., Hu, B., Suib, S., Raymond, D. & Li, B. 2011. A pilot-scale study on utilizing multi-anode/cathode microbial fuel cells (MAC MFCs) to enhance the power production in wastewater treatment. International Journal of Hydrogen Energy 36, pp. 876-884.

[21] Li, J., Ge, Z. & He, Z. 2014. A fluidized bed membrane bioelectrochemical reactor for energy-efficient wastewater treatment. Bioresource Technology 167, pp. 310-315.

[22] Kim, K-Y., Yang, W. & Logan, B. 2015. Impact of electrode configurations on retention time and domestic wastewater treatment efficiency using microbial fuel cells. Water Research 88, pp. 41-46.

[23] Mäkinen, A. E., Nissilä, M. E. & Puhakka, J. A. 2012. Dark fermentative hydrogen production from xylose by a hot spring enrichment culture. International Journal of Hydrogen Energy 37, 17, pp. 12234-12240.

[24] Logan, B. E., Hamelers, B., Rozendal, R., Schröder, U., Keller, J., Freguia, S., Aelterman, P., Verstraete, W. & Rabaey, K. 2006. Microbial Fuel Cells: Methodology and Technology. Environmental Science and Technology 40, 17, pp. 5181-5192.

[25] Dubois, M., Gilles, K. A., Hamilton, J. K., Rebers, P. A. & Smith, F. 1956. Colorimetric Method for Determination of Sugars and Related Substances. Analytical Chemistry 28, 3, pp. 350-356

[26] van Haandel, A. & van der Lubbe, J. 2007. Handbook biological waste water treatment. Design and optimization of activated sludge systems, Quist Publishing, Leidschendam.

[27] Koskinen, P. E. P., Kaksonen, A. H. & Puhakka, J. A. 2007. The relationship Between the Instability of H2 Production and Compositions of Bacterial Communities Within a Dark Fermentation Fluidized-Bed Bioreactor. Biotechnology and Bioengineering 97, 4, pp. 742-758.

[28] Muyzer, G., de Waal E.C. & Uitterlinden A.G. 1993. Profiling complex microbial populations by denaturing gradient gel electrophoresis analysis of polymerase chain reaction-amplified genes coding for 16 S rRNA. Applied and Environmental Microbiology 59, 3. pp. 695-700.

[29] Muyzer, G., Hottenträger, S., Teske, A. & Waver C. 1996. Denaturing gradient gel electrophoresis of PCR-amplified 16S rRNA – a new molecular approach to analyse the genetic diversity of mixed microbial communities. In: Akkermans ADL, van Elsas JD, de Bruijn F. (eds) , Molecular microbial ecology manual. Kluwer, Dordrecht, pp. 3.4.4/1-23.

[30] Lakaniemi, A-M., Hulatt, C. J., Thomas, D. N., Tuovinen, O. H. & Puhakka, J. A. 2011. Biogenic hydrogen and methane production from *Chlorella vulgaris* and *Dunaliella tertiolecta* biomass. Biotechnology for Biofuels 4, 34.

[31] Ieropoulos, I., Winfield, J. & Greenman, J. 2010. Effects of flow-rate, inoculum and time on the internal resistance of microbial fuel cells. Bioresource Technology 101, pp. 3520-3525.

[32] Shen, L., Ma, J., Song, P., Lu, Z., Yin, Y., Liu, Y., Cai, L. & Zhang, L. 2016. Anodic concentration loss and impedance characteristics in rotating disk electrode microbial fuel cells. Bioprocess and Biosystems Engineering 39, 10, pp. 1627-1634.

[33] Kim, J., Boghani, H., Amini, N., Aguey-Zinsou, K-F., Michie, I., Dinsdale, R., Guwy, A., Guo, Z. & Premier, G. 2012. Porous anodes with helical flow pathways in bioelectrochemical systems: The effect of fluid dynamics and operating regimes. Journal of Power Sources 213, pp. 382-390.

[34] Sevda, S., Chayambuka, K., Sreekrishnan, T.R., Pant, D., Dominguez-Benetton, X. 2015. A comprehensive impedance journey to continuous microbial fuel cells. Bioelectrochemistry 106, pp. 159-166.

[35] Kostamo, A., Holmbom, B. & Kukkonen, J. 2004. Fate of wood extractives in wastewater treatment plants at kraft pulp mills and mechanical pulp mills. Water Research 38, pp. 972-982.

[36] Requeiro, L., Lema, J. & Carballa, M. 2015. Key microbial communities steering the functioning of anaerobic digesters during hydraulic and organic overloading shocks. Bioresource Technology, 197, pp. 208-216.

[37] Beecroft, N.J., Zhao, F., Varcoe, J.R., Slade, R.C.T, Thumser, A.E. & Avignone-Rossa, C. 2012. Dynamic changes in the microbial community composition in microbial fuel cells fed with sucrose. Applied Microbiology and Biotechnology 93, 1, pp. 423-437.

[38] Morotomi, M., Nagai, F. & Watanabe, Y. 2012. Description of *Christensenella minuta* gen. nov., sp. nov., isolated from human faeces, which forms a distinct branch in the order *Clostridiales*, and proposal of *Christensenellaceae* fam. nov. International Journal of Systematic and Evolutionary Microbiology, 62, pp. 144-149.

[39] Lin, C-Y. & Cheng, C-H. 2006. Fermentative hydrogen production from xylose using anaerobic mixed microflora. International Journal of Hydrogen Energy, 31, 7, pp. 832-840.

[40] Wei, L., Yan, Z., Cui, M., Han, H., Shen, J. 2012. Study on electricity-generation characteristic of two-chambered microbial fuel cell in continuous flow mode. International Journal of Hydrogen Energy, 37, 1, pp. 1067-1073.

[41] Salinas, M. B., Fardeau, M-L., Cayol, J-L., Casalot, L., Patel, B., Thomas, P., Garcia, J-L. & Ollivier, B. 2004. *Petrobacter succinatimandens* gen. nov., sp. nov., a moderately thermophilic, nitrate-reducing bacterium isolated from an Australian oil well. International Journal of Systematic and Evolutionary Microbiology, 54, pp. 645-649.

[42] Chen, S. & Dong, X. 2005. *Proteiniphilum acetatigenes* gen. nov., sp. nov., from a UASB reactor treating brewery wastewater. International Journal of Systematic and Evolutionary Microbiology, 55, pp. 2257-2261.

[43] Keevil, C. W., Hough, J. S. & Cole, J. A. 1977. Prototrophic Growth of *Citrobacter freundii* and the Biochemical Basis for its Apparent Growth Requirements in Aerated Media. Journal of General Microbiology 98, pp. 273-276.

[44] Biddle, A., Leschine, S., Huntemann, M., Han, J., Chen, A., Kyrpides, N., Markowitz, V., Palaniappan, K., Ivanova, N., Mikhailova, N., Ovchinnicova, G., Schaumberg, A., Pati, A., Stamatis, D., Reddy, T., Lobos, E., Goodwin, L., Nordberg, H., Cantor, M., Hua, S., Woyke, T. & Blanchard, J. 2014. The complete genome sequence of *Clostridium indolis* DSM 755 T. Standards in Genomic Sciences 9, pp. 1089-1104.

[45] Huang, L., Zhu, N., Cao, Y., Peng, Y., Wu, P. & Dong, W. 2015. Exoelectrogenic bacterium phylogenetically related to *Citrobacter freundii*, isolated from anodic biofilm of a microbial fuel cell. Applied Biochemistry and Biotechnology 175, 4, pp. 1879-1891.

[46] Sun, D., Wang, A., Cheng, S., Yates, M. & Logan, B. 2014. *Geobacter anodireducens* sp. nov., an exoelectrogenic microbe in bioelectrochemical systems. International Journal of Systematic and Evolutionary Microbiology, 64, pp. 3485-3491.

548 [47] Sun, Y., Wei, J. Liang, P. & Huang, X. 2011. Electricity generation and microbial
549 community changes in microbial fuel cells packed with different anodic materials.
550 Bioresource Technology 102, 23, pp. 10886-10891.
551
552 [48] Wang, S., Huang, L., Gan, L., Quan, X., Li, N., Chen, G., Lu, L., Xing, D. & Yang, F.
553 2012. Combined effects of enrichment procedure and non-fermentable or fermentable co-
554 substrate on performance and bacterial community for pentachlorophenol degradation in
555 microbial fuel cells. Bioresource Technology 120, pp. 120-126.
556
557 [49] Cord-Ruwisch, R., Lovley, D. & Schink, B. 1998. Growth of *Geobacter*
558 *sulfurreducens* with Acetate in Syntrophic Cooperation with Hydrogen-Oxidizing
559 Anaerobic Partners. Applied and Environmental Microbiology 64, 6, pp. 2232-2236.
560